ERA

Submitted to Journal of Nuclear
Instruments and Methods

UCRL-19892
Preprint

A STUDY ON THE CHOICE OF PARAMETERS FOR A HIGH ENERGY ELECTRON RING ACCELERATOR

C. Bovet and C. Pellegrini

June 26, 1970

AEC Contract No. W-7405-eng-48

UCRL-19892

ERAN-73
UCRL-19892

A STUDY ON THE CHOICE OF PARAMETERS FOR A HIGH ENERGY ELECTRON RING ACCELERATOR

C. Bovet and C. Pellegrini

Lawrence Radiation Laboratory
University of California
Berkeley, California

June 26, 1970

ABSTRACT

The production of high energy (multi-GeV) proton beams by an electron ring accelerator is considered. Both the final energy and intensity of the proton beam depend on the choice of parameters for the electron ring. Possible sets of parameters, consistent with all the known requirements of ring stability, and which optimize the energy and (or) the intensity of the proton beam, are presented.

A STUDY ON THE CHOICE OF PARAMETERS FOR A HIGH ENERGY ELECTRON RING ACCELERATOR*

C. Bovet† and C. Pellegrini‡

Lawrence Radiation Laboratory
University of California
Berkeley, California

June 26, 1970

1. Introduction

The design of an electron ring accelerator (ERA), intended to accelerate protons in the multi-GeV region, is quite different from that of a synchrotron.[1] In the last case the only important parameters that must be chosen in order to have a certain final energy and intensity are the machine radius aperture and injection energy. By contrast, in the ERA case, the final proton energy not only depends on the total accelerating voltage but also depends critically on the ratio of ion to electron numbers in the ring and on the geometry of the ring itself.

Another important difference is that the physics of a proton synchrotron is well documented, both theoretically and experimentally, but this is not yet the case for an ERA. In fact, although we know that electron rings can be formed and compressed and the Dubna group has shown that ions can be accelerated,[2] many important aspects of an ERA still await clarification. For instance, the stability of an electron-ion ring under the effect of an accelerating force is still not completely understood. The same is true for the amount of coherent energy loss from the ring in crossing the accelerating cavities. Experimental information on these points is certainly much needed before a (real) detailed design of a multi-GeV ERA can be done.

However, we think that it is still interesting, on the basis of what we already know and by using reasonable assumptions on what we do not know completely, to try to design an ERA and to understand how the various parameters determine the final machine performance.

---

* This work was initiated as a basis for a section of "Conceptual Studies for New Technology Proton Accelerators (50-100 GeV)" published by the staff, Accelerator Study Group, LRL, Berkeley, Calif., April 7, 1970, to which we are referring for a discussion of the technological feasibility.

† Permanent address: CERN, Geneva, Switzerland.

‡ Permanent address: Laboratori Nazionali di Frascati [illegible]

The scheme of the ERA considered is the following (fig. 1). The transition from the initial state, labeled 1, just after injection, to the final state, 5, which is the proton beam at maximum energy, is assumed to occur in four different stages.

From state 1 to state 2, the ring is compressed in a varying magnetic field. From state 2 to state 3 the ring is further compressed by synchrotron radiation to the final compressed state.

Subsequently, the ring is loaded with protons and accelerated by means of an electric field, in a column of length L_e, to reach a state called 4. The final state, 5, is obtained through magnetic expansion in a solenoid of length L_m.

All the formulas used to put restraints on the ring parameters in order to obtain a stable ring are collected in section 2.

Since, for a given length of the electric and magnetic accelerating column, the final ion energy and intensity depend essentially on the ring parameters in the compressed state, we have first optimized the ring parameters in state 3 (section 3).

Afterwards, we have studied what type of compressor is needed to form the ring (section 4). In section 5 we discuss the numerical results obtained.

2. Conditions for Ring Stability

To evaluate what kind of performance can be expected from an ERA we require that a number of conditions be satisfied by the ring parameters, which are the number of electrons N_e, the ring radius R, the ring radial and axial radii a and b, and the ion loading f, which is the ratio of ion to electron numbers. The conditions are essentially stability conditions for the ring during the whole process of ring formation and acceleration.

The first condition we use is that the square of the axial betatron frequency ν_z^2 (measured in units of revolution frequency), must always be positive. This is normally satisfied during ring compression, but could be violated near the end of compression and in the acceleration column, where the field index, n, is equal to zero. For n = 0 the condition

$\nu_z^2 > 0$ can be written as [3]

$$\nu_z^2 = \frac{4\mu R^2}{b(a+b)}\left(f - \frac{1}{\gamma_\perp^2}\right) - (1-f)\frac{\mu P}{2} + \mu\left[\frac{\epsilon_m}{(S_m-1)^2} - \frac{(1-f)\epsilon_e}{(S_e-1)^2}\right] > 0, \qquad (2.1)$$

where

$$\mu = \frac{N_e r_e}{2\pi R \gamma_\perp}, \qquad (2.2)$$

$$P = 2\,\ell n\,[16R/(a+b)], \qquad (2.3)$$

ϵ_e, ϵ_m are the electrostatic and magnetostatic image field coefficients, S_e and S_m are the ratio of the radius of the cylinder for electrical or magnetic images to the ring major radius, r_e is the classical electron radius, and $\gamma_\perp$ the ratio of total energy to rest mass energy for the electrons in the reference frame where the ring is at rest. In eq. (2.1) the term proportional to $R^2 f/b(a+b)$ describes the ion focusing effect and the term proportional to $1/\gamma_\perp^2$ describes the electron space-charge forces. This last term is corrected for the effect of curvature of the electron beam by the term proportional to P.

The condition that $\nu_z^2 > 0$ can be written as in (2.1) only under the assumption that during the acceleration process the ions stay in the ring. In fact, to write eq. (2.1) we assume that both electrons and ions are uniformly distributed inside the same elliptical ring cross section. It is clear that this can be true only when the external accelerating force is zero. In the presence of an external accelerating force the electron and ion distributions will be modified and a polarization will appear. We will assume that, to a first approximation and for the cases when ions are not lost from the ring, eq. (2.1)holds when the ring is accelerated. A consistent solution to the problem of the polarized ring is not at hand, but some simplified models[4,5] give estimates of the maximum acceleration the ring can undergo without losing the ions. Under such circumstances the effective holding power $e\mathcal{E}_H$ is

smaller than the maximum holding power, $e\mathcal{E}_{H,max.}$, calculated for totally overlapping uniform distribution of ions and electrons, by a factor $1/\eta$

$$e\mathcal{E}_H = \frac{1}{\eta}\, e\mathcal{E}_{H,max.} = \frac{1}{\eta}\,\frac{2\, N_e r_e\, mc^2}{\pi\,(a+b)\,R}\,. \tag{2.4}$$

The requirement that the radial betatron frequency, ν_r, be positive is usually always satisfied and introduces no real limitations. But near the end of the compression cycle or when the ring is moved into the accelerating column, ν_r can cross the value 1. As has been discussed by Pellegrini and Sessler,[6] the crossing of the integral resonance can give rise to an increase in the minor ring dimensions. In order to maintain this increase within tolerable limits, one requires that the ratio of frequency spread in the ring, $\Delta\Omega$, to the frequency shift due to the ions, be much less than one. This can be written as

$$\frac{\Delta\Omega^2}{\omega_o^2} \ll \frac{4\,\mu\, R^2 f}{a(a+b)} + \frac{\mu\, P f}{2}$$

or

$$\frac{\Delta\Omega^2}{\omega_o^2} \ll \frac{2\, N_e r_e R\, f}{\pi\, a(a+b)\gamma_\perp}\left(1 + \frac{1}{8}\,\frac{a(a+b)}{R^2}\,P\right) \tag{2.5}$$

where $\Omega = w\omega_o$ and ω_o is the revolution frequency. Usually this condition is well satisfied when we are below the threshold for the resistive wall instability (see Eqn. (2.6)).

For the resistive wall instability we can estimate the threshold, N_w, assuming that the Landau damping is the stabilizing mechanism. In this case the threshold is determined roughly by the condition that the frequency spread $\Delta\Omega_z$ is of the same order as the coherent frequency shift due to space-charge forces

$$\frac{\Delta\Omega_z^2}{\omega_o^2} \approx \frac{2N_w r_e R}{\pi\gamma_\perp b(a+b)} \left\{ \frac{1}{\gamma_\perp^2} + \epsilon\frac{b(a+b)}{\gamma_\perp^2 h^2} + \frac{1}{8}\frac{b(a+b)}{R^2} P \right\} . \tag{2.6}$$

For the negative mass case, when neglecting the effect of coherent radiation negative mass instability is neglected [7], the threshold is given by

$$N_m = \frac{\pi}{2}\frac{R}{r_e}\frac{\gamma_\perp}{g}\frac{1}{1-n}\left(\frac{\Delta p}{p}\right)^2 , \tag{2.7}$$

where $\frac{\Delta p}{p}$ is the electron total momentum spread and

$$g = \frac{1}{\gamma_\perp^2}\left(1 + 2\,\ell n\,\frac{2h}{\pi a}\right) + \left(\frac{h}{\pi R}\right)^2 \qquad \text{if } h \ll R \tag{2.8}$$

or

$$g = \frac{1}{\gamma_\perp^2}\left(1 + 2\,\ell n\,\frac{8R}{a}\right) \qquad \text{if } R \ll h, \tag{2.9}$$

where h is the distance from the ring to the walls, which are now assumed to be planes orthogonal to the axis of the ring. N_e must also be below the limit N_c for incoherent space-charge effect. This limit can be written as

$$N_c = \frac{\pi\,\nu_z\overline{\Delta\nu}_z\gamma_\perp}{r_e R}\left\{\frac{1}{b(a+b)\gamma_\perp^2} + \frac{\epsilon}{h^2}\right\}^{-1} , \tag{2.10}$$

or

$$N_c = \frac{\pi\,\nu_r\overline{\Delta\nu}_r\gamma_\perp}{r_e R}\left\{\frac{1}{a(a+b)\gamma_\perp^2} + \frac{\epsilon}{h^2}\right\}^{-1} , \tag{2.11}$$

where ϵ is an image field coefficient, usually $\epsilon \approx 0.2$, h is the distance from the ring to the conducting wall, and $\overline{\Delta\nu}_{z,r}$ is the allowed frequency shift. In (2.10), (2.11) we assumed no ion present in the ring.

(See Page 5A)

Other limitations on the ring parameters can be due to the instabilities associated with the ion-electron interactions.[8] These interactions seem to be dangerous when the ion oscillates in the potential well created by the electrons, with a frequency near to the electron cyclotron frequency. In this paper we will not consider these possible limitations, although in the range of ring parameters that will result from the numerical computation the ion oscillation frequency is of the same order of magnitude of the electron cyclotron frequency, thus leading to a potentially dangerous situation.

3. Optimum Ring

Optimum means giving rise to a maximum number of ions N_i accelerated to a top energy E_5, together with the following restrictions:

(i) ν_z must be greater than 0, produced by ion focusing without image focusing during the electric acceleration, but with image focusing in the magnetic expansion,

(ii) the holding power $e\mathcal{E}_H$ must be larger than the rate of energy gain $\frac{dE}{dz}$ of the ions for them to keep within the ring during electric and magnetic acceleration,

(iii) the number of electrons N_e must be below the thresholds for space charge, negative mass, and resistive wall instabilities, the last being by far the most severe restriction in the compressed state.

We now list a series of assumptions and formulae that will form a closed set of relations for the fairly large number of parameters involved.

The optimum is not a strong function of the ring minor radii ratio a/b, therefore we can assume that the injection procedure will lead to equal betatron amplitudes in the radial and axial planes,

$$a_\beta = b. \tag{3.1}$$

Let us introduce a parameter k for the ratio of the amplitudes associated with the energy spread to the betatron oscillation amplitudes,

$$k = a_s/a_\beta , \tag{3.2}$$

It has been shown that the rms value of the transverse beam distribution is of primary significance for the maximum field[9] (giving rise to the holding power). Since betatron and energy spread amplitudes are uncorrelated, we shall further make use of a radial beam size given by

$$a = (a_\beta^2 + a_s^2)^{\frac{1}{2}} \tag{3.3}$$

Axial focusing

In the electric acceleration there will be no image focusing because of the large aperture of the cavities necessary to reduce the ring radiative energy loss. In order to keep a reasonable focusing we ask for

$\nu_z^2 = \frac{2\mu R^2}{b(a+b)} \left(f - \frac{1}{\gamma_\perp^2}\right)$, so that from (2.1) one obtains

$$f - \frac{1}{\gamma_{\perp 3}^2} = \frac{b(a+b)}{4R^2} P, \tag{3.4}$$

On the other hand, during magnetic expansion a conical vacuum chamber may be designed so that the image wall effect is important (of the order of μP). We therefore assume that the magnetic expansion may be performed until the Coulomb defocusing just equals the ion focusing, i.e.,

$$\gamma_{\perp 5} = 1/f^{\frac{1}{2}} . \tag{3.5}$$

Instability thresholds

The resistive wall threshold proves to be the more restrictive constraint in the compressed stage. Since n = 0, the frequency spread is esentially due to $\Delta p/p$. We express $\Delta p/p$ in terms of the synchrotron amplitude so that from (2.6) we obtain

$$N_w = \frac{2\pi\gamma_\perp}{r_e} \frac{a_s b(a+b)}{R^2} \left\{ \frac{1}{\gamma_\perp^2} + \frac{\epsilon(a+b)b}{h^2\gamma_\perp^2} + \frac{1}{8} \frac{b(a+b)}{R^2} P \right\}^{-1}.$$

In this formula we neglect the image term, which is very small in the electric column, and we use eq. (3.4) to substitute for the third term in the bracket, so that

$$N_w = \frac{4\pi}{r_e} \frac{a_s b(a+b)}{R^2} \gamma_\perp \left\{ f + \frac{1}{\gamma_\perp^2} \right\}^{-1}, \tag{3.6}$$

It is clear that we should not allow the number of electrons N_e to be $> N_w$. On the other hand values of $N_e < N_w$ might give rise to different families of rings presenting some interesting properties. We shall describe these families with the parameter $\mu > 1$ such that

$$N_e = N_w/\mu . \tag{3.7}$$

Ring acceleration

The holding power we have already discussed in section 2 (eq. 2.4):

$$e\mathcal{E}_H = \frac{2\, N_e\, r_e\, mc^2}{\pi\, \eta(a+b)\, R} \quad . \tag{3.8}$$

In the electric acceleration we assume $\eta_e = 4$; in the magnetic expansion we use $\eta_m = 2$ because image focusing there adds to the holding power.

The energy gained by the ions in the electric acceleration is

$$\frac{dE_i}{dz} = \frac{M}{m\gamma_\perp} \frac{1-f}{1+g}\, e\, \mathcal{E}_x(1-\alpha\, N_e), \tag{3.9}$$

where $g = f \frac{M}{m\gamma_\perp}$, and the bracket accounts for the cavity radiation.

The problem of the cavity radiation is not yet completely solved, especially the dependence of the energy loss on γ.[10] We have used numerical values of α computed by Keil;[11] α proved to be very sensitive to the cavity bore radius, which must then be made large enough compared with the ring major radius.

From eqs. (3.8) and (3.9) one obtains the requirement for holding power:

$$\frac{2\, N_e r_e\, mc^2}{\pi\, \eta_e (a+b) R} = \frac{M}{m\gamma_\perp} \frac{1-f}{1+g}\, e\, \mathcal{E}_x(1-\alpha N_e) \quad . \tag{3.10}$$

In the axial magnetic field B, R, and $\gamma_\perp$ are approximately related by the cyclotron equation

$$BR = \frac{e}{c} \rho_\perp = e\, \beta_\perp\, \gamma_\perp\, m, \tag{3.11}$$

so that all our variables a, a_β, a_s, b, N_w, N_e, R, $\gamma_\perp$, and f are now related by the set of eqs. (3.1) through (3.4), (3.6), (3.7), (3.10), and (3.11); only one of them is a free parameter (we chose the loading fraction f).

The ion energy E_4 at the end of electric acceleration is just given by integrating eq. (3.9) over the length L_e:

$$E_4 = Mc^2 + \frac{M}{m\gamma_\perp} \frac{1-f}{1+g}\, e\, \mathcal{E}_x(1-\alpha\, N_e) L_e. \tag{3.12}$$

Then during the magnetic expansion, the canonical angular momentum conser-

vation in the moving frame and the conservation of the total energy lead to the relation (see Appendix A)

$$\Gamma = \frac{\gamma_{\parallel 5}}{\gamma_{\parallel 4}} = \frac{1+g}{\gamma_{\perp 5}/\gamma_{\perp 4}+g} , \tag{3.13}$$

which gives the final ion energy

$$E_5 = \Gamma E_4 . \tag{3.14}$$

An interesting point to make[12] is that this final energy depends only upon the effective accelerating voltage $V_{eff} = \mathcal{E}_x(1-\alpha N_e)L_e$ and the final transverse energy of the electrons $\gamma_{\perp 5}$, when $f \ll 1$ and $Mc^2 \ll E_4$ are neglected. Using the final transverse energy given by eq. (3.5), one has

$$E_5 \approx \frac{M/m}{1/f^{\frac{1}{2}} + f\ M/m}\ e\ V_{eff}, \tag{3.15}$$

which reaches a maximum for $f = (m/2M)^{2/3} \approx 0.004$.

The length L_m needed for magnetic expansion is (see Appendix A)

$$L_m = \frac{2\eta_m \lambda(1+g)\gamma_{\parallel 4}}{g^3}\left[(1-k^{\frac{1}{2}})\left(\frac{1}{k^{\frac{1}{2}}} + \frac{1}{(g+k^{\frac{1}{2}})(g+1)}\right) + 2\,\ell n\left(\frac{(g+1)k^{\frac{1}{2}}}{g+k^{\frac{1}{2}}}\right)\right], \tag{3.16}$$

where η_m is the derating of the holding power ($\eta_m = 2$ is used in the numerical calculation), $\lambda = \pi R_4(a_4+b_4)M/(4 N_e m r_e)$, and

$$\kappa = \frac{B_5}{B_4} = \left(\frac{\gamma_{\perp 5}\ \beta_{\perp 5}}{\gamma_{\perp 4}\ \beta_{\perp 4}}\right)^2 \approx \left(\frac{\gamma_{\perp 5}}{\gamma_{\perp 4}}\right)^2 , \tag{3.17}$$

since $\beta_{\perp 5} \approx \beta_{\perp 4}$.

For $0 < z < L_m$ eq. (3.16) also gives an implicit function $B_4 < B(z) < B_5$, which must be satisfied by the solenoid field.

For the numerical results that follow, we considered two different limitations on the expansion: i) the expansion is limited by the axial focusing (eq. 3.5) and L_m is given by eq. (3.16) (in some cases with large $\gamma_{\perp 4}$ this will result in unreasonably large values of L_m), (ii) on top of the focusing condition we put $L_m \leq L$, where L has been chosen for a given accelerator. In both cases we assume that the optimum function $B(z)$ may be achieved in the expansion solenoid. Note that the image focusing produced by the conical vacuum chamber in the expansion column will not be optimum for different ring radii R_4.

4. Compression process

We want now to determine the parameters of the ring at injection as a function of the compressed (final) ring parameters (state 3) such that the number of electrons always stays below the thresholds N_w, N_m, and N_c.

The transformation that leads from the initial to the final state is assumed to consist of a magnetic compression from an initial value B_1 to an intermediate value B_2 of the magnetic field, followed by a synchrotron radiation compression.[13] The synchrotron radiation occurs in a constant-gradient magnetic field, characterized by a field index n_3. We also allow for the possibility that during the magnetic compression the magnetic flux linked with the ring and the value of the magnetic field on the ring orbit can be changed in an independent way.

The transformation leading from the initial state, labeled by the subscript 1, to the intermediate state, 2, and to the final compressed state, 3, can be characterized by three parameters,

$$\rho_{12} = B_2/B_1 , \tag{4.1}$$

$$\xi = 1 + \frac{\phi_2 - \phi_1}{2\pi B_1 R_1^2} , \tag{4.2}$$

$$\sigma = \frac{R_2}{R_3} \equiv \left(1 - \frac{2}{3} r_e c \frac{3n_3 - 1}{1 - n_3} \frac{\gamma_{\perp 2}^3}{R_2^2} t \right)^{1/(1 - 3n_3)} , \tag{4.3}$$

where ϕ_i is the magnetic flux linked with the ring in the state i,

and σ describes the effect of synchrotron radiation. The case

$$\rho_{12} = 1, \quad \sigma = 1$$

corresponds to a static compressor[14], in which the electron energy is constant, and the case

$$\rho_{12}/\xi = 1, \quad \sigma = 1$$

corresponds to the case of a betatron, in which the ring major radius is constant. The relation between the initial and final parameters of the electron ring are derived in Appendix B, and are summarized here:

$$R_1 = \left(\frac{\rho_{12}}{\xi}\right)^{\frac{1}{2}} \sigma R_3 , \tag{4.4}$$

$$p_{\perp 1} = (\rho_{12}\ \xi\ )^{-\frac{1}{2}} \sigma^{1-n_3}\ p_{\perp 3} , \tag{4.5}$$

$$B_1 = \rho_{12}^{-1} \sigma^{-n_3} B_3 , \tag{4.6}$$

$$a_{\beta 1} = \rho_{12}^{\frac{1}{2}} \sigma^{n_3/2} a_{\beta 3} , \tag{4.7}$$

$$a_{s1} = \frac{1-n_3}{1-n_1} (\xi\rho_{12})^{\frac{1}{2}} \sigma^{2-3n_3} a_{s3} , \tag{4.8}$$

$$\left.\frac{\Delta p_\perp}{p_\perp}\right)_1 = \sigma^{1-3n_3}\ \xi\ \left.\frac{\Delta p_\perp}{p_\perp}\right)_3 , \tag{4.9}$$

where a_β, a_s are the betatron and synchrotron amplitudes and $\Delta p_\perp/p_\perp$ is the momentum spread.

Using eqs. (4.4), $\cdots$, (4.9), one can evaluate the ring parameters during the whole transformation leading from state 3 to state 1, and also evaluate, using eqs. (4.10),$\cdots$, (4.16), the thresholds N_w, N_m, and N_c. It is thus possible to study the stability of the ring during the compression process.

It is interesting to show that, for any set of compressed ring parameters, there exists a range of parameters ρ_{12}, ξ, σ such that the stability conditions are all satisfied. To simplify the calculations

we assume that for N_w and N_c, the most restricting conditions are those referring to the axial direction (this is justified by the fact that $b < a$), i.e., eqs. (3.6) and (2.10). We also assume that for N_m we can use eq. (2.7) with g defined by (2.8). We will also neglect, wherever possible, the terms deriving from curvature or image effects. These thresholds can then be written as

$$N_w = \frac{\pi(\Delta\Omega_z^2/\omega_o^2)}{2r_e}\ \gamma_\perp^3\ R\ \frac{b(a+b)}{R^2}\quad , \tag{4.10}$$

$$N_m = \frac{\pi\ R\ \gamma_\perp^3}{2r_e(1-n)(1+2\ \ell n\ \frac{2h}{\pi a})}\ \left(\frac{\Delta p}{p}\right)^2\quad , \tag{4.11}$$

$$N_c = \frac{\pi\ \nu_z\overline{\Delta\nu}_z}{r_e}\ \gamma_\perp^3\ R\ \frac{b(a+b)}{R^2}\quad . \tag{4.12}$$

Assuming also $\nu_z\overline{\Delta\nu}_z > \frac{\Delta\Omega_z^2}{2\omega_o^2}$, we can neglect (4.12), which is less restrictive than (4.10).

The thresholds N_w and N_m can now be written as a function of the ring parameters in state 3 and of ρ_{12}, ξ, σ:

$$N_w = \frac{\pi\ \Delta\Omega_z^2/\omega_o^2}{2r_e}\ \gamma_{\perp 3}^3\ R_3\left(\frac{b_3}{R_3}\right)^2\ \xi^{-1}\rho_{12}^{-1}\sigma^{2-2n_3}\cdot$$

$$\left\{1 + \left[1 + k^2\left(\frac{1-n_3}{1-n_1}\right)^2\ \xi\ \sigma^{4-7n_3}\right]^{\frac{1}{2}}\right\}\quad , \tag{4.13}$$

$$N_m = \frac{2\pi}{r_e}\ \frac{1-n_1}{(1+2\ \ell n\ \frac{2h}{\pi a})}\ R_3\gamma_{\perp 3}^3\left(\frac{b_3}{R_3}\right)^2\ k^2$$

$$\left(\frac{1-n_3}{1-n_1}\right)^2\ \rho_{12}^{-1}\ \sigma^{6-9n_3}\quad . \tag{4.14}$$

The number of electrons in the ring can be obtained from (3.6), and (3.7), so that the condition for stability is equivalent to satisfying the two inequalities

$$\frac{\Delta\Omega_z^2}{\omega_o^2}\,\frac{\sigma^{2-2n_3}}{\xi\,\rho_{12}}\left\{1+\left[1+k^2\left(\frac{1-n_3}{1-n_1}\right)^2\xi\,\sigma^{4-7n_3}\right]^{\frac{1}{2}}\right\}\geq \frac{8}{\mu}\,\frac{b_3}{R_3}\,\frac{k\left[1+(1+k^2)^{\frac{1}{2}}\right]}{1+\gamma_{\perp 3}^2 f}\,, \qquad (4.15)$$

$$\frac{(1-n_1)}{1+2\,\ell n\,\frac{2h}{\pi a}}\left(\frac{1-n_3}{1-n_1}\right)^2 k\,\frac{\sigma^{6-9n_3}}{\rho_{12}}\geq\frac{2}{\mu}\,\frac{b_3}{R_3}\,\frac{1+(1+k^2)^{\frac{1}{2}}}{1+\gamma_{\perp 3}^2 f}\,. \qquad (4.16)$$

Assuming

$$\frac{\Delta\Omega_z^2}{\omega_o^2}\approx 0.1,$$

$$1+2\,\ell n\,\frac{2h}{\pi a}\approx 3,$$

$$n_3\approx 0,$$

$$n_1\approx\frac{1}{2}\,,$$

$$k=2,$$

$$1+\gamma_{\perp 3}^2 f\approx 5\,,$$

we obtain approximately from (4.16) and (4.15) respectively

$$\frac{\sigma^6}{\rho_{12}}\geq\frac{1}{\mu}\,\frac{b_3}{R_3}\,, \qquad (4.17)$$

$$\frac{\sigma^2}{\rho_{12}\xi}\left[1+(1+16\,\xi\,\sigma^4)^{\frac{1}{2}}\right]\geq\frac{10^4}{\mu}\,\frac{b_3}{R_3}\,. \qquad (4.18)$$

These conditions are satisfied during the synchrotron radiation compression (from state 2 to state 3), i.e., for $\xi = 1$, $\rho_{12} = 1$, $\sigma \geq 1$.

During the transformation from state 1 to state 3 we must satisfy the inequalities which follow from (4.17) and (4.18),

$$\rho_{12} \leq \sigma^6 \mu / \frac{b_3}{R_3} , \tag{4.19}$$

$$\xi \leq \frac{\mu\sigma^2}{52 \frac{b_3}{R_3}} \frac{1}{\rho_{12}} + \frac{\mu\sigma^6}{13\, \rho_{12}^2 \frac{b_3}{R_3}} , \tag{4.20}$$

where ξ is a function of $\rho_{12} = \frac{B}{B_1}$ with $B_1 \leq B \leq B_3$.

In order to make more explicit these conditions on ξ, let us introduce for ρ_{12} a scaled variable

$$x = \frac{1}{\mu\sigma^2} \frac{b^3}{R_3} \rho_{12} . \tag{4.21}$$

The preceding inequalities now read

$$x \leq \sigma^4 ,$$

$$\xi \leq \frac{1}{52}\left(\frac{1}{x} + \frac{\sigma^4}{13} \frac{1}{x^2}\right) , \tag{4.23}$$

and fig. 2 represents the available domain for $\xi(x)$.

Tuning of the compressor to meet various machine performances

For an existing machine some of the parameters are fixed: the injection radius R_1 into the compressor, maybe also the injection energy and therefore B_1, and also the compressed radius $R_3 = R_4$ if the magnetic acceleration requires image focusing.

Furthermore, the ratio $\frac{b_3}{R_3}$ is not a function of B_3 nor of μ, as one can check on fig. 3 and 4. When the machine is driven to the optimum performance the loading fraction is rather close to $f = 1\%$ (see fig. 7). We shall then assume in the following analytical approach that

$\frac{b_3}{R_3}$ is fixed. B_3, μ, and σ will remain the free parameters, large B_3 and small μ giving rise to the maximum energy E_5, whereas small B_3 and high μ produce the largest intensity. Equation (4.6) is applied to substitute ρ_{12} into eq. (4.19), which becomes

$$\mu \sigma^6 \geq \frac{B_3}{B_1} \frac{b_3}{R_3} , \tag{4.24}$$

and using also eq. (4.4) one gets for eq. (4.20)

$$\left(\frac{b_3}{R_3} \frac{R_3}{R_1} \frac{B_3}{B_1} \right)^2 \leq \frac{\mu}{52} \left(\frac{b_3}{R_3} + \frac{\mu \sigma^6}{13} \frac{B_1}{B_3} \right). \tag{4.25}$$

When a choice of values is made for μ and σ, which satisfies both eq. (4.24) and (4.25), ξ is determined by eq. (4.4) and (4.6), so that

$$\xi = \left(\frac{R_3}{R_1} \right)^2 \frac{B_3}{B_1} \sigma^2 . \tag{4.26}$$

Here again ξ as a function of ρ_{12} must satisfy the inequality (4.20) during the compression. The betatron amplitude at injection is given by eq. (4.7), so that

$$b_1 = (\rho_{12})^{\frac{1}{2}} b_3 . \tag{4.27}$$

The requirements (4.24) and (4.25) are most difficult to meet when $B_3 = B_{3\,max}$. For lower values of B_3 there is more flexibility, ξ increases which is favorable but b_1 decreases. B_3 is bounded towards small values by the space-charge limit.

5. Numerical Results

a. Optimum ring

The set of equations expressed in sect. 3 can be solved for different values of the parameter f, by use of numerical iteration. Some parameters have been given fixed values:

$$k = 2,$$

$$\eta_e = 4,$$

$$\eta_m = 2,$$

$$\mathcal{E}_x = 5 \text{ MV/m},$$

$$\alpha = 1/6 .$$

Different values of k have been tried; k = 2 was definitely better than k = 1, but larger values did not improve the performances significantly and resulted in too small betatron amplitude. The n values have been discussed in Section 3. The external accelerating field $\mathcal{E}_x$ has been suggested by the present ERA development at Berkeley. There is some chance that this value can be increased by future development,[15] resulting in improved machine performances. For the radiation of the ring passing through the cavities we took the best numerical estimate presently available,[11] corresponding to cavity base radius of 19 cm and ring radius R = 1 to 3 cm.

Some other parameters are variable in the following range:

$$0{\cdot}2\,\% < f < 4\%$$

$$\mu = 1 \text{ or } 2.5,$$

$$B = 15,\ 20,\ 30 \text{ kG}.$$

The curves on fig. 3 and 4 show N_i, B_3, and b_3/R_3 as functions of the loading fraction f, for $\mu = 1$ and $\mu = 2.5$ respectively.

With all the constraints used in the optimization, a solution exists only over a certain range of values for f. Too low f-values clearly do not provide enough ion focusing; at the other extreme too large values of f do not allow one to meet all the requirements. N_i will be discussed when displayed as a function of the top energy E_5 in fig. 7.

For any value of μ, B, and f the major radius R_3 of the optimum ring lies between 1 and 3 cm. It is nevertheless a rather strong function of f, since a factor 4 up in f requires a factor 2 down in R_3. The axial minor radius b_3 of the ring is only a few per cent of the major radius R_3.

We shall now show an example of accelerating column which we worked out for a "conceptual study" at Berkeley. The total length at our disposal was $L_t = 470$ m, but some of the results that are presented below for this example can be scaled with the length of the accelerator. We optimized the performances versus cost, considering that 1 m of electric acceleration column was three times as expensive as 1 m of magnetic expansion column,[16] and arrived at $L_e = 320$ m.

In figs. 5 and 6 the total acceleration length L_t, the maximum energy E_5, and the ratio of total to electric acceleration Γ are plotted for the same range of the variable parameter. Solid lines represent performances that can be achieved with $L_m \leq 150$ m, dashed lines correspond to longer machines. Without any constraint on L_m, the maximum of E_5 would be reached in the region of $f = 0.004$, as foreseen in the simplified analysis of section 3.

The performances of the accelerator are shown on fig. 7 in an intensity-energy diagram. Solid lines represent the range of optimum performance for a given μ and different B values. The dashed curves represent rings with different loading fractions f (f = 1% is marked by a black dot).

b. Case of fixed initial and final ring radius

In the foregoing discussion of the optimum ring all the initial and final ring parameters were determined only by the ring stability conditions. In particular, the geometrical characteristics, such as the ring radius at injection and in the electric and magnetic accelerating columns, change with the final energy and intensity. For a given compressor and a given electric column and expansion solenoid, it is convenient to keep R_1 and R_4 fixed, still satisfying the stability conditions. The performance of such a machine is illustrated in figs. 8 and 9, for the case $R_1 = 50$ cm, $R_2 = 2$ cm.

In fig. 8 we give the final energy, E_5, and number of ions, N_i, as a function of the magnetic field, B_3, in the electric accelerating column, for $\mu = 1$ and 2.5. The time needed for radiation compression is given for some of the points on the curves. Injection energy, E_1, current, I, and betatron amplitude, b_1, are given in fig. 9. The injection current

is evaluated with a single-turn injection process assumed; this value might be considerably reduced by the use of spiral injection.[17] We have also assumed that the compression parameter ξ is fixed and equal to 0.1.

To evaluate the ring parameters at injection, we used (2.6), (2.7), (2.8), and (2.10), assuming the betatron frequency spread and shift to be given by

$$\frac{\Delta \Omega_z^2}{\omega_o^2} \approx 0.1, \quad \nu_z \overline{\Delta \nu}_z \approx 0.1.$$

The value of h has been adjusted for each case in the interval $2.5 \text{ cm} < h < 8 \text{ cm}$ so as to optimize the thresholds.

It is interesting to notice that to obtain high energies, we need high magnetic fields and small betatron amplitude at injection. However, in this case the injection energy increases and the injection current decreases, so that the needed brightness of injected beam tends to remain constant over the considered range of B_3.

c. Pulse to pulse fluctuations

The compressed electron ring will not be perfectly reproducible from pulse to pulse, with the consequence that the performances of the machine will fluctuate around mean values. Pulse-to-pulse fluctuations of the intensity is well known for synchrotrons and is of no harm as long as it amounts to only a few per cent. For the ERA this means that the loading fraction f must be stable within such a limit. But, the most striking fact with the ERA is that the maximum energy E_5 is not only a function of the external fields but also of the ring properties. How strong is this dependence has been established by numerical differentiation for the machine treated on fig. 9, with $\mu = 2.5$. The order of magnitude of these coefficients is as follows:

Parameters (par)	R_1	E_1	N_e	$\frac{B_2}{B_1}$	ξ	t	f
$\frac{\text{par}}{E_5} \quad \frac{\Delta E_5}{\Delta(\text{par})}$	$-\frac{1}{10}$	$-\frac{1}{2}$	$-\frac{1}{2}$	$-\frac{1}{5}$	$-\frac{1}{3}$	$-\frac{1}{15}$	$-\frac{1}{3}$

This shows that energy fluctuations of the order of 10^{-2} will be observed, which is in the range of the intrinsic energy spread.[18]

APPENDIX

A. Magnetic Expansion

Before magnetic expansion, the ring is in state 4 with a transverse momentum $\beta_{\perp 4}\gamma_{\perp 4}$ mc and an axial velocity $\beta_{\parallel 4}$ c.

In the frame moving with the ring, the conservation of the canonical angular momentum may therefore be expressed as

$$\frac{(\gamma_\perp \beta_\perp)^2}{(\gamma_{\perp 4} \beta_{\perp 4})^2} = \frac{B}{B_4} = \kappa, \qquad \text{(A-1)}$$

where nonsubscripted variables are functions of z during the expansion. Through a Lorentz transformation the total energy of an electron in the lab system is seen to be

$$\gamma = \gamma_\parallel \gamma_\perp . \qquad \text{(A-2)}$$

Thus, the energy conservation for the whole ring reads

$$\gamma_\parallel (\gamma_\perp N_e m + N_i M) = \gamma_{\parallel 4}(\gamma_{\perp 4} N_e m + N_i M), \qquad \text{(A-3)}$$

which leads to

$$\frac{\gamma_\parallel}{\gamma_{\parallel 4}} = \frac{1+g}{(\gamma_\perp/\gamma_{\perp 4}) + g}, \qquad \text{(A-4)}$$

where $g = N_i M/(N_e m \gamma_{\perp 4})$.

Using (A-1) and (A-4), we get

$$\frac{\gamma_\parallel}{\gamma_{\parallel 4}} = \frac{1+g}{k^{\frac{1}{2}} (\beta_{\perp 4}/\beta_\perp) + g} . \qquad \text{(A-5)}$$

According to eq. (3.8) the accelerating force that might be applied to the ions is given by

$$\frac{dE_i}{dz} = \frac{2N_e m c^2 r_e}{\pi \eta_m R(a+b)} . \qquad \text{(A-6)}$$

In the expansion solenoid one may assume that the magnetic field is uniform in r although it varies very slowly with z. The transformation laws for R, a, and b are then given by eq. (4.4), (4.7), and (4.8) with $\xi = \sigma = 1$, $n_1 = n_3 = 0$, and $\rho_{12} = \kappa$, so that

$$\frac{dE}{dz} = \frac{4\, N_e\, m\, r_e}{\pi\, \eta_m R_4 (a_4 + b_4) M} \frac{Mc^2 \kappa}{2} = \frac{Mc^2 \kappa}{2\eta_m \lambda} , \qquad (A\text{-}7)$$

where $\lambda = \pi\, R_4 (a_4 + b_4)\, M/(4\, N_e\, m\, r_e)$.

Equating the acceleration of the ions to their accelerating force gives

$$\frac{d\gamma_{\parallel}}{dz} = \frac{1}{Mc^2} \frac{dE_i}{dz} = \frac{\kappa}{2\eta_m \lambda} . \qquad (A\text{-}8)$$

The derivative of (A-5) is

$$\frac{d\gamma_{\parallel}}{dz} = -\frac{1}{2} \frac{\gamma_{\parallel 4}(1+g)\, \beta_{\perp 4}/\beta_{\perp}}{(k^{\frac{1}{2}} \beta_{\perp 4}/\beta_{\perp} + g)^2\, k^{\frac{1}{2}}} \frac{d\kappa}{dz} , \qquad (A\text{-}9)$$

which expression, combined with (A-8), gives

$$\frac{d\kappa}{dz} = -\frac{\beta_{\perp 4}/\beta_{\perp}}{\eta_m \lambda\, (1+g)\, \gamma_{\parallel 4}} \kappa^{3/2} (k^{\frac{1}{2}} + g\, \beta_{\perp}/\beta_{\perp 4})^2 . \qquad (A\text{-}10)$$

[This expression is similar to eq. (14) of Lewis,[19] which was derived in the case in which $\gamma_4 = 1$.]

Equation (A-10) may now be integrated to give a relationship between z and κ,

$$z = \frac{2\, \eta_m \lambda\, (1+g)\, \gamma_{\parallel 4}}{g h^2} \left[h(1-\sqrt{\kappa})\, \frac{1}{k^{\frac{1}{2}}} + \left(\frac{1}{(h+1)(h+k^{\frac{1}{2}})} \right) + 2\, \ell n \left(\frac{(h+1)}{h + k^{\frac{1}{2}}} \right) \right] , \qquad (A\text{-}11)$$

where $h = g\, \beta_{\perp}/\beta_{\perp 4}$.

Equation (A-11) gives an explicit solution for the length L of the expansion column when κ is fixed, and may be used, in turn, for fixing the values of B(z) in the solenoid.

B. Magnetic Compression

For an electron in an axially symmetric magnetic field the generalized azimuthal momentum,

$$P_\theta = m\gamma_\perp r v_\theta - \frac{e}{c} r A_\theta, \tag{B-1}$$

is conserved. We further have a relationship between the radius of the trajectory, the field, and the momentum, namely

$$p_\perp c = e B r. \tag{B-2}$$

Using (B-1), (B-2), and the relation between the vector potential and the flux,

$$\phi \equiv \phi(B) = \int_S \underline{B} \cdot \underline{n}\, dS = \oint A \cdot ds = 2\pi r A_\theta, \tag{B-3}$$

we obtain

$$Br^2 - \frac{\phi}{2\pi} = \text{const}, \tag{B-4}$$

which may also be written

$$R_2^2 = R_1^2 \frac{B_1}{B_2}\left(1 + \frac{\phi_2 - \phi_1}{2\pi R_1^2 B_1}\right), \tag{B-5}$$

or, defining ξ and ρ_{12} as

$$\left.\begin{aligned} \xi &= 1 + \frac{\phi_2 - \phi_1}{2\pi R_1^2 B_1}, \\ \rho_{12} &= B_2/B_1, \end{aligned}\right\} \tag{B-6}$$

$$R_2 = R_1 \left(\frac{\xi}{\rho_{12}}\right)^{\frac{1}{2}}. \tag{B-7}$$

For relativistic particles, the momentum transformation law follows immediately from (B-2), i.e.,

$$p_{\perp 2} = (\rho_{12}\, \xi)^{\frac{1}{2}}\, p_{\perp 1}. \tag{B-8}$$

To obtain the transformation law for betatron amplitudes we use the adiabatic invariant $p/R\ \nu\ a_\beta^2 = \text{constant}$, from which it follows, for the radial and vertical betatron amplitudes,

$$a_{\beta 2} = a_{\beta 1}\ \rho_{12}^{-\frac{1}{2}} \left(\frac{1-n_1}{1-n_2}\right)^{\frac{1}{4}}, \qquad \text{(B-9)}$$

$$b_2 = b_1\ \rho_{12}^{-\frac{1}{2}} \left(\frac{n_1}{n_2}\right)^{\frac{1}{4}} . \qquad \text{(B-10)}$$

In section 4, eq. (4.7), we have neglected the small changes in betatron amplitude due to the change in n between states 1 and 2, so that we can use only one formula for the transformation law of radial and vertical betatron amplitudes. To obtain the transformation law for the synchrotron amplitude we use the invariant (B-4). For a particle having an energy $p_\perp + \Delta p_\perp$ and radius $R + \Delta R$, we have, from (B-2),

$$c\,\Delta p_\perp = (1-n)\ eB\,\Delta R, \qquad \text{(B-11)}$$

and from (B-4)

$$2\,RB\Delta R + R^2\Delta B - \frac{\Delta\phi}{2\pi} = \text{constant}. \qquad \text{(B-12)}$$

But, for a field B which near the orbit changes like $B \propto R^{-n}$, we have

$$\Delta B = -n\,B R^{-1}\Delta R \qquad \text{(B-13)}$$

and

$$\frac{\Delta\phi}{2\pi} = R\,B\,\Delta R\ . \qquad \text{(B-14)}$$

From (B-11),$\cdots$, (B-14), it follows that

$$R\Delta p_\perp = \text{constant},$$

or

$$R_1\,\Delta p_{\perp 1} = R_2\,\Delta p_{\perp 2}\ . \qquad \text{(B-15)}$$

Inserting in (B-15) the transformation laws for R and $p_\perp$, (B-7), and (B-8), we finally obtain

$$\frac{\Delta p_{\perp 1}}{p_{\perp 1}} = \xi \frac{\Delta p_{\perp 2}}{p_{\perp 2}} . \qquad \text{(B-16)}$$

The total transformation from state 1 to 3 is obtained by considering the synchrotron radiation effect between states 2 and 3. The formulas describing the change in the ring parameters under the effect of radiation are derived in reference (13), to which we refer the reader for details.

Acknowledgements

We wish to thank all the members of the Accelerator Study Group of the Lawrence Radiation Laboratory, Berkeley, for their hospitality and for their continued interest in this work; we also gratefully acknowledge many stimulating discussions with D. Keefe and A.M. Sessler.

REFERENCES

1. D. Keefe, Particle Accelerators, 1, 1 (1970).
2. V. P. Sarantsev, in Proceedings of the VII International Conference on High Energy Accelerators, Erevan, USSR, 1969 (to be published).
3. L. J. Laslett (Lawrence Radiation Laboratory, Berkeley, California), ERA internal report ERAN-30 (1969).
4. L. Smith, private communication.
5. C. Pellegrini, unpublished notes.
6. C. Pellegrini and A. M. Sessler, Crossing of an Incoherent Integral Resonance in the Electron Ring Accelerator, UCRL-19462 (1970) (submitted to Nucl. Instr. Methods).
7. C. Pellegrini and A. M. Sessler, in Symposium on Electron Ring Accelerators held at Lawrence Radiation Laboratory, Berkeley, California, UCRL-18103 (1968), p. 442.
8. F. E. Mills, in Symposium on Electron Ring Accelerators held at Lawrence Radiation Laboratory, Berkeley, California, UCRL-18103 (1968), p. 448. T.K. Fowler, in Symposium on Electron Ring Accelerators held at Lawrence Radiation Laboratory, Berkeley, California, UCRL-18103 (1968), p. 457.
9. C. Bovet (Lawrence Radiation Laboratory, Berkeley, California), ERA Internal Report, ERAN-88 (1970).
10. R.D. Hezeltine, M. N. Rosenbluth, and A. Sessler, UCRL-19793.
11. E. Keil, private communication.
12. D. Keefe, private communication.
13. C. Pellegrini, UCRL-19815 (May, 1970).
14. L. J. Laslett and A. M. Sessler, A Method for Static-Field Compression in an Electron-Ring Accelerator, UCRL-18589 (1969).
15. E. Hartwig, private communication.
16. W. Salsig, private communication.
17. C. Bovet (Lawrerence Radiation Laboratory, Berkeley, California), ERA Internal Report ERAN-87 (1970).
18. D. Keefe, in Symposium on Electron Ring Accelerators held at Lawrence Radiation Laboratory, Berkeley, California, UCRL-18103 (1968), p. 79.
19. W. B. Lewis, in Symposium on Electron Ring Accelerators held at Lawrence Radiation Laboratory, Berkeley, California, UCRL-18103 (1968), p. 195.

Figure Captions

Fig. 1. Schematic layout of an electron ring accelerator.

Fig. 2. During compression the variation of the flux linkage ξ must stay below a certain limit in order to avoid ring instabilities.

Fig. 3. Optimum compressed ring parameters. The number of protons N_i, major radius R_3, and minor radius b_3 are plotted as functions of the loading fraction f, for different values of the magnetic field B. The number of electrons in the ring is just at the threshold for instabilities ($\mu = 1$).

Fig. 4. Optimum compressed ring parameters. The number of protons N_i, major radius R_3, and minor radius b_3 are plotted as functions of the loading fraction f, for different values of the magnetic field B. The number of electrons in the ring is below the threshold for instabilities by a factor $\mu = 2.5$.

Fig. 5. Optimum ring. Final proton energy E_5, total machine length L_t, and ratio of total to electric acceleration Γ are plotted as functions of the loading fraction f, for different values of the magnetic field B. The number of electrons in the ring is just at the threshold for instabilities ($\mu = 1$).

Fig. 6. Optimum ring. Final proton energy E_5, total machine length L_t, and ratio of total to electric acceleration Γ are plotted as functions of the loading fraction f, for different values of the magnetic field B. The number of electrons in the ring is below the threshold for instabilities by a factor $\mu = 2.5$.

Fig. 7. Optimum performance of an ERA with 320 m of electric acceleration and 150 m of magnetic acceleration. The number of protons in the ring N_i is plotted versus their final energy E_5, for different values of the magnetic field B. The number of electrons in the ring is below the threshold for instabilities by a factor $\mu = 1$ and 2.5. Black circles correspond to f = 1% and arrows show the direction of increasing loading.

Fig. 8. Performance of an ERA with fixed ring radius at injection, $R_1 = 0.5$ m, and in compressed state, $R_3 = 2$ cm. Number of protons N_i and their final energy E_5 are plotted versus the magnetic field level B, for different electron-threshold-to-intensity ratio $\mu = 1$ to 2.5. Some of the compression is obtained by radiation.

Fig. 9. Injected beam quality. Energy E_1, intensity I, and betatron amplitude b_1 of the injected beam are plotted versus B, magnetic field in the accelerating column for an ERA with fixed ring radii $R_1 = 0.5$ m and $R_3 = 2$ cm. Two different values are considered for the electron-threshold-to-intensity ratio ($\mu = 1$ and 2.5).

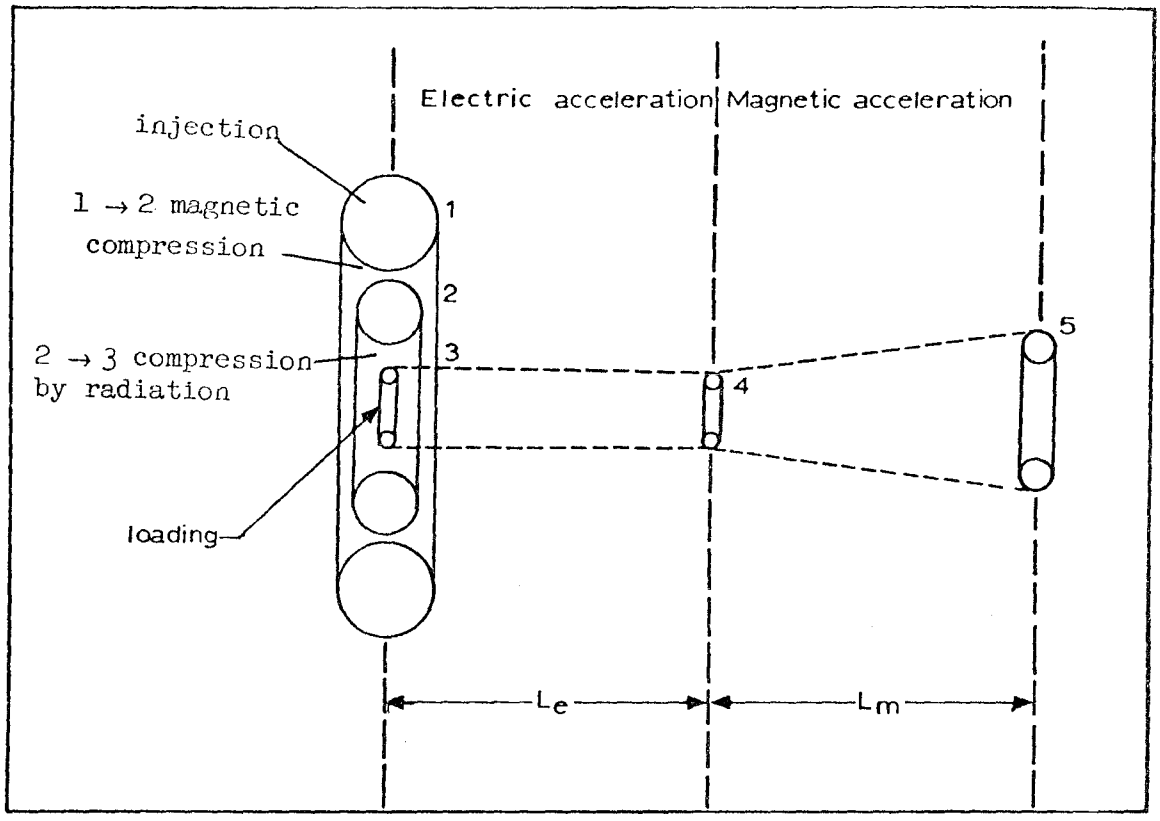

XBL 705 6201

Fig. 1

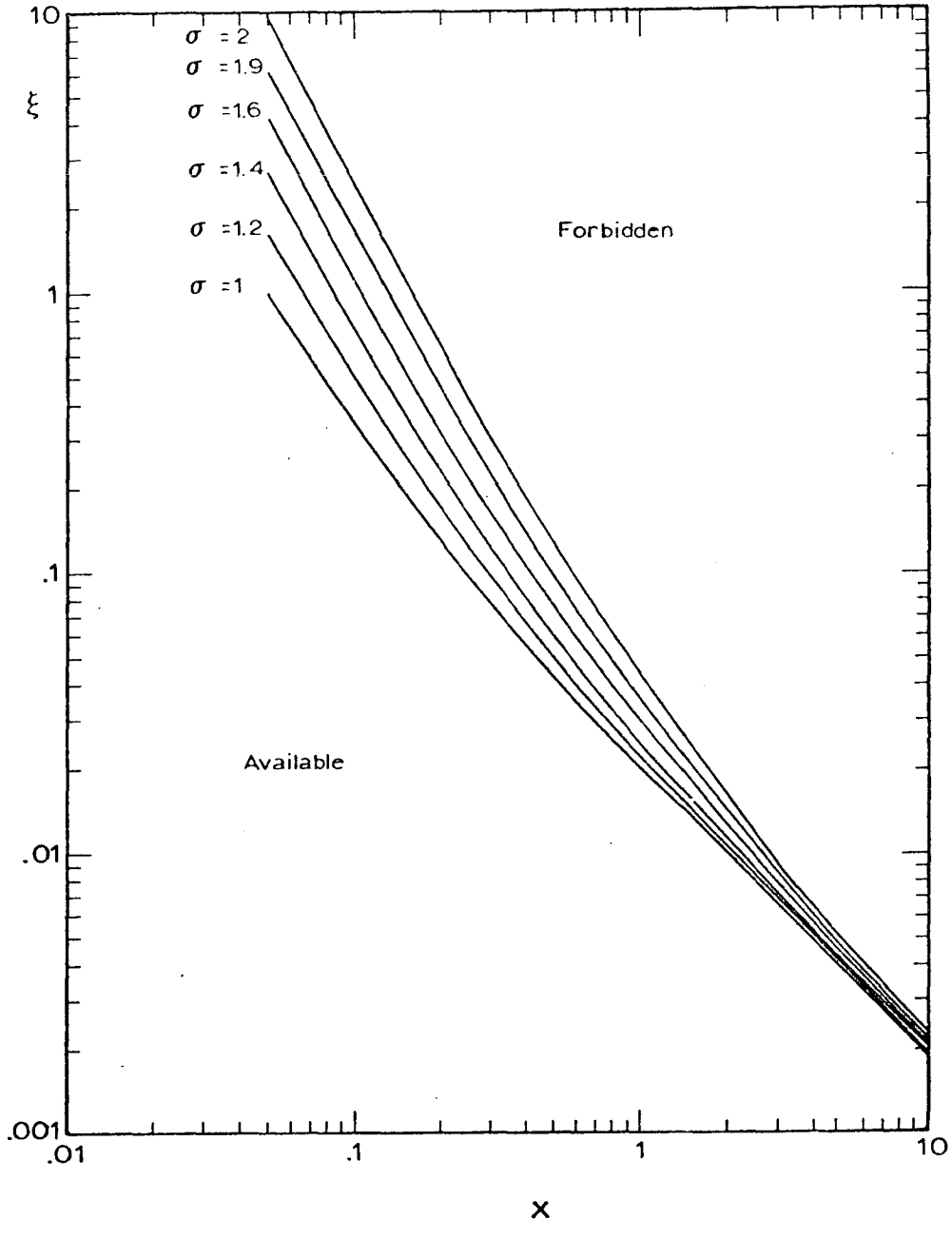

XBL 705 6202

Fig. 2

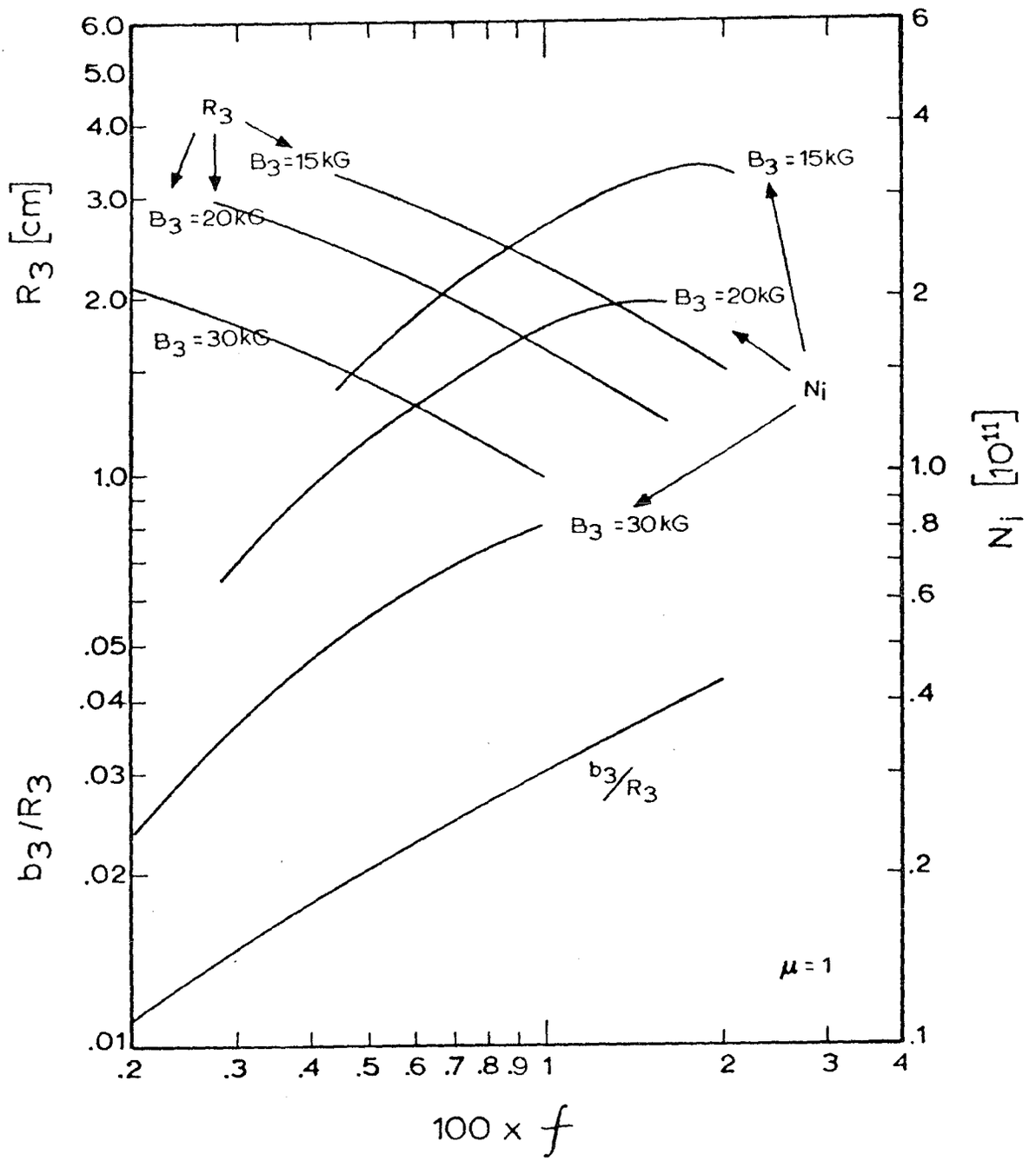

XBL 705 6203

Fig. 3

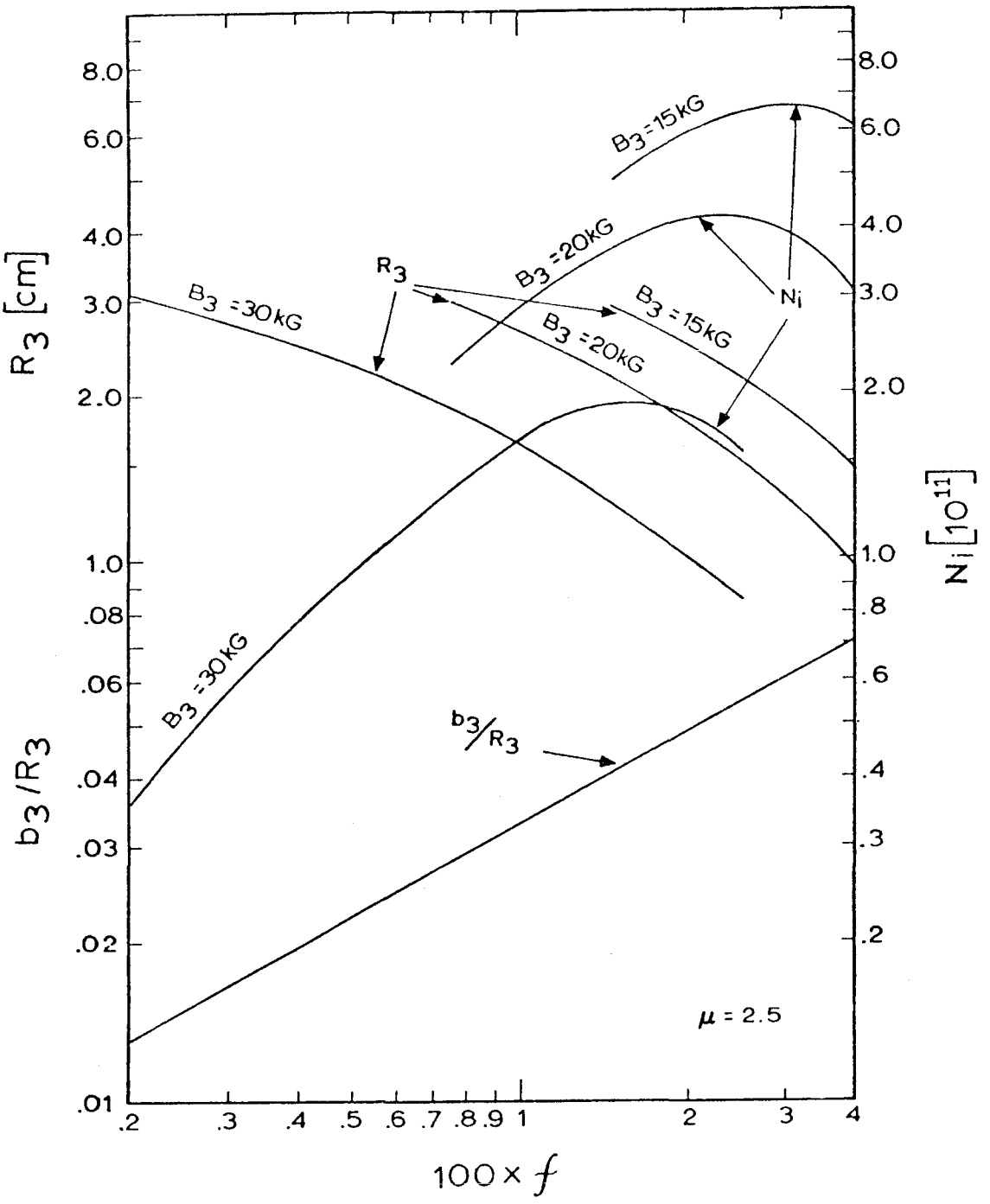

XBL 705 6204

Fig. 4

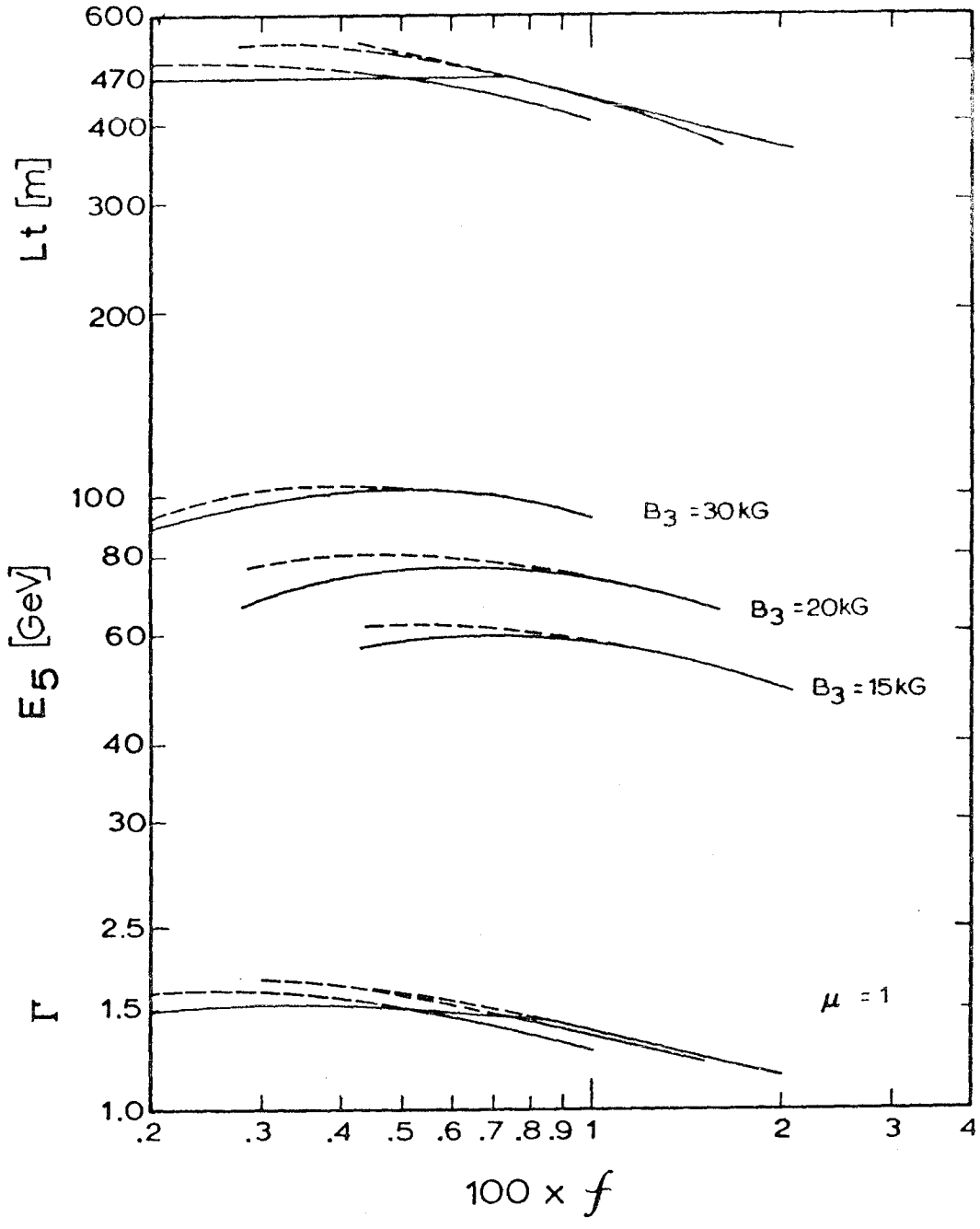

XBL 705 6205

Fig. 5

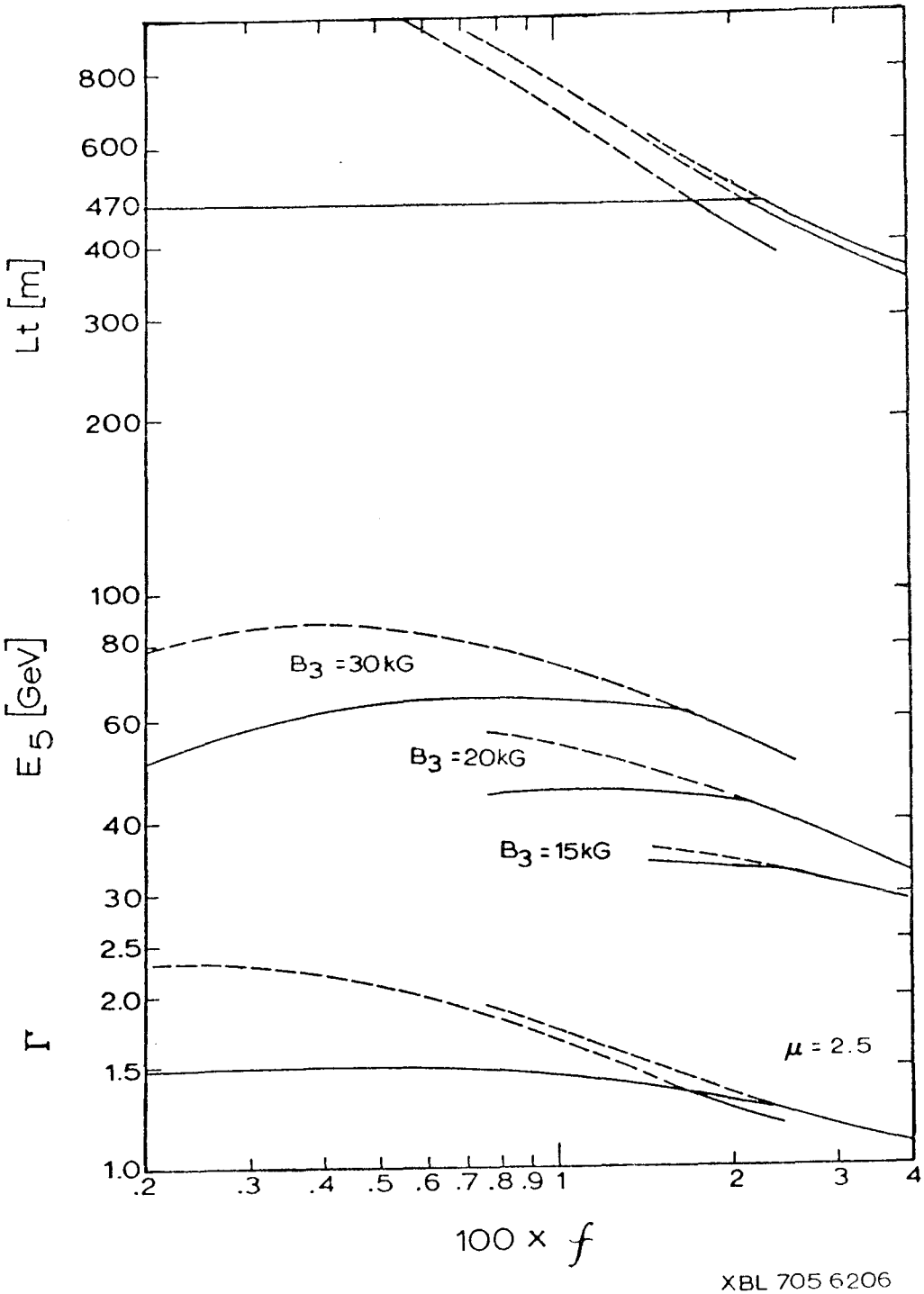
800
600
470
400
300
200
Lt [m]
100
80
60
40
30
2.5
2.0
1.5
1.0
E5 [GeV]
Γ
B3 =30kG
B3 =20kG
B3 =15kG
μ = 2.5
.2
.3
.4
.5
.6
.7
.8
.9
1
2
3
4
100 x f
XBL 705 6206

Fig. 6

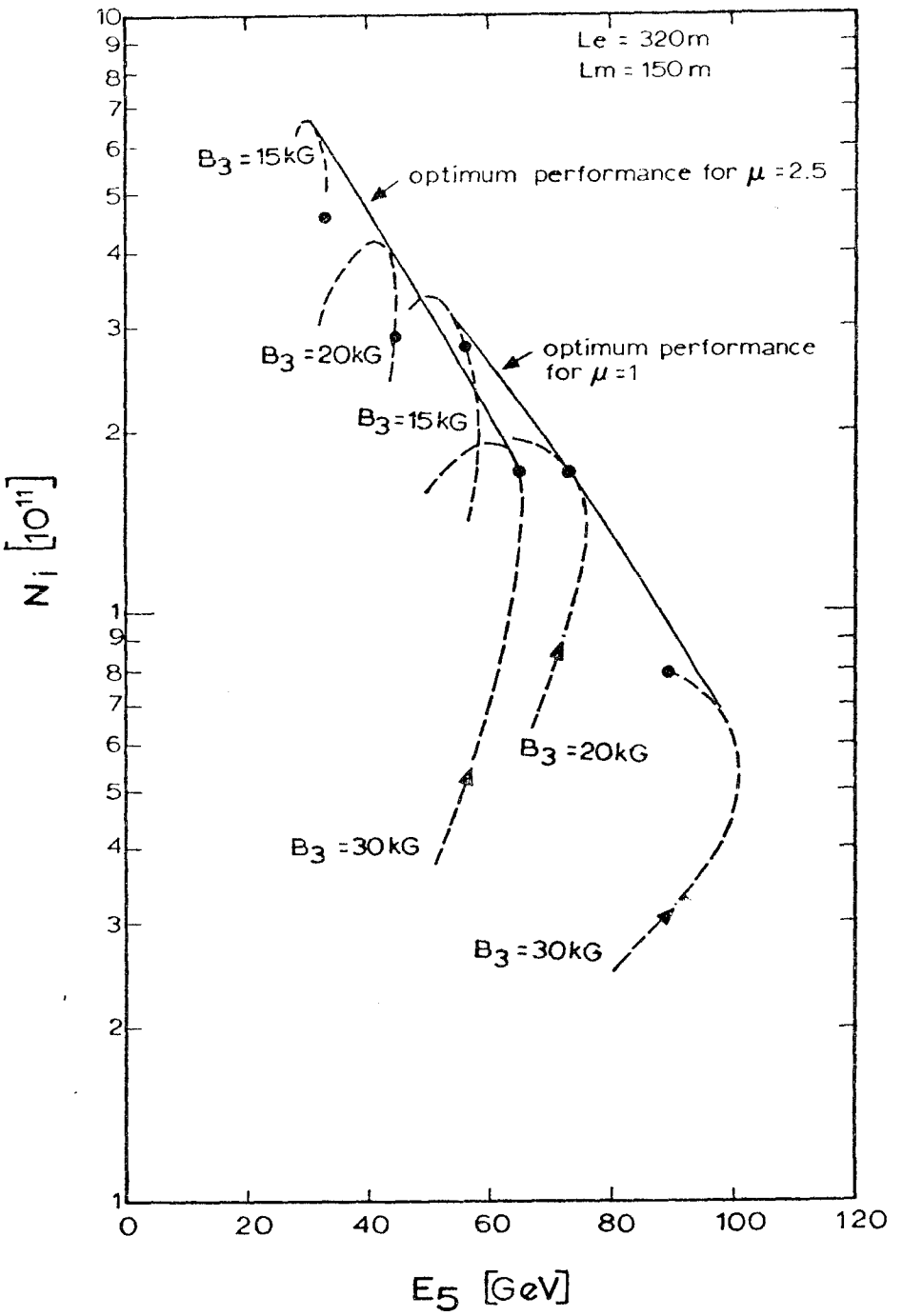

XBL 705 6207

Fig. 7

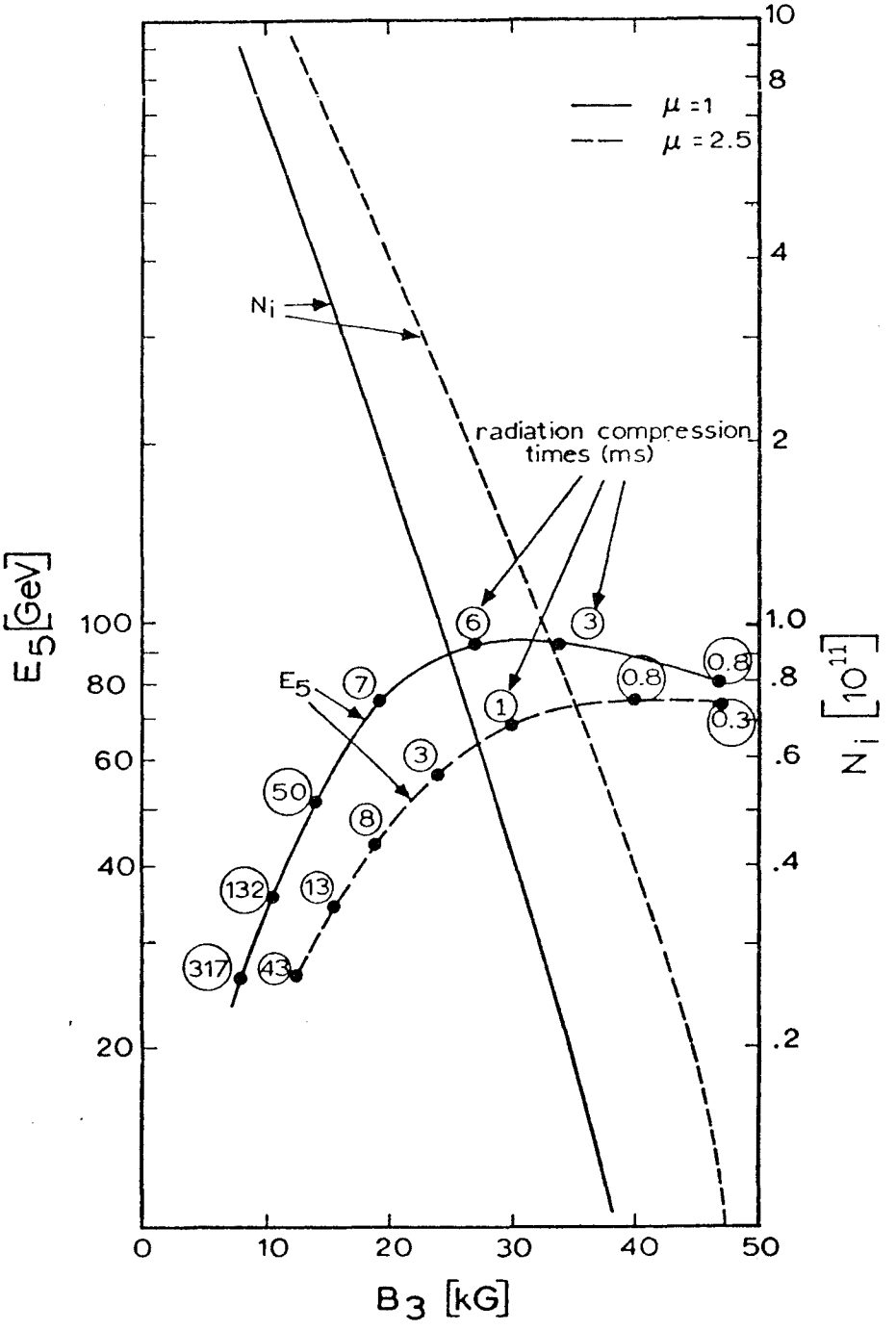

XBL 705 6208

Fig. 8

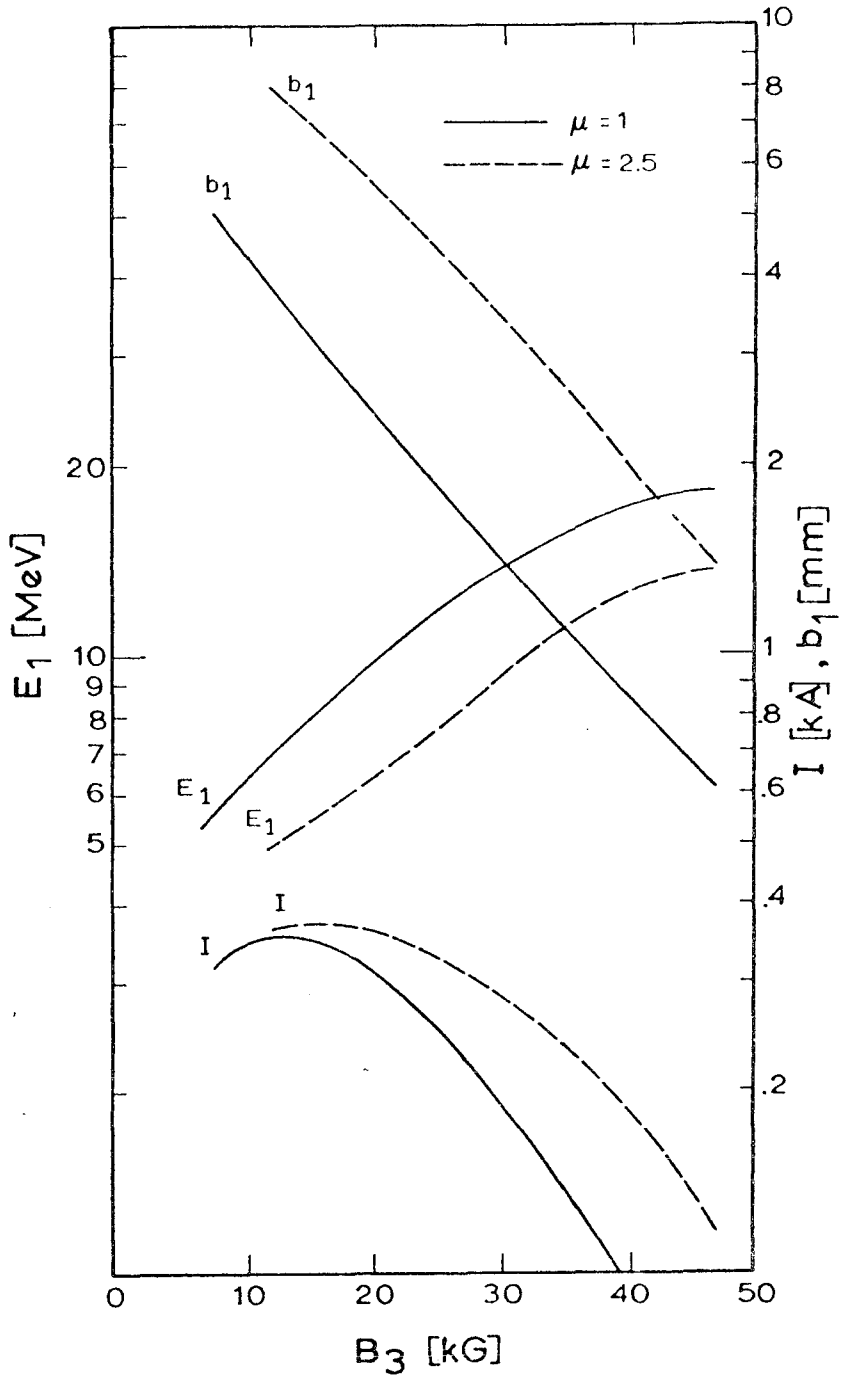

XBL 705 6209

Fig. 9